Barium-stabilized $Sr_2Al_xSi_{12-x}N_{16-x}O_{x+2}$:Eu Green Phosphor for White Light UVLED

Wenjie Xie, Yachong Wang, Xin Xu,* and Chusheng Chen
Laboratory of Advanced Functional Materials and Devices, Department of Materials Science and Engineering,
University of Science and Technology of China, Hefei 230026, P. R. China

(Received January 23, 2008; CL-080076; E-mail: xuxin@ustc.edu.cn.)

We discovered the stabilization effect of only 1 wt % Ba on synthesizing Eu^{2+}-doped pure Sr–S-phase($Sr_2Al_xSi_{12-x}N_{16-x}O_{x+2}$) under a moderate condition and studied their luminescent properties. The excitation band is at UV–vis spectral region which is about 300–370 nm, and the emission band at 508–538 nm. The emission wavelength changes from 508 to 538 nm as a function of Eu^{2+} concentration, and the maximum emission intensity could be obtained with the Eu^{2+} concentration of 0.2. This phosphor can be the potential candidate for using as the green phosphor for UVLED-based white light.

The ultraviolet light-emitting diode (LED)-based white light is sweeping allover our life. It has many advantages in superior lifetime, efficiency, reliability, designable, and low pollution form fossil fuel. A primitive method of making white light is to mix light from red-, green-emitting phosphors and blue LED chips or to mix light from red-, green-, and blue-emitting phosphors and UVLED.[1,2] Recently, rare-earth-activated oxynitride phosphors have attracted much attention because of their advantages of better flexibility, composition-tunable and higher thermal stability.[3–5] The Sr–S phase ($Sr_2Al_xSi_{12-x}N_{16-x}O_{x+2}$) was first reported in 1995, it was a new phase that coexists with α-SiAlON and β-SiAlON in Sr-doped system, and then the research showed that Ba–S phase also exists.[6] But the luminescent properties of this new phase and potential application as functional material have not been studied. In this paper, we synthesized the Eu^{2+}-doped $Sr_2Al_xSi_{12-x}N_{16-x}O_{x+2}$ under a moderate condition and simple method through the stabilization of Ba and then studied their luminescent properties.

The Eu^{2+}-doped $M_2Al_xSi_{12-x}N_{16-x}O_{x+2}$ ($M = Sr$, Ba, $x = 2$ in this study) samples were synthesized with Eu_2O_3, $BaCO_3$, $SrCO_3$, Si_3N_4, AlN, Al_2O_3, and SiO_2 powders by a solid-state reaction method. After weighed out stoichiometrically, all the powders were milled in a Si_3N_4 mortar. The resulting mixtures were fired in BN crucibles at N_2 atmosphere for about 2 h at 1650 °C.

The phase was analyzed by an X-ray diffractometer (XRD, Philips PW 1700) using Cu Kα radiation at a scanning rate of 0.5 degree/min. The photoluminescence spectra were measured by a fluorescent spectrophotometer (F-4500, Hitachi Ltd.).

Figure 1 is XRD patterns of three samples, all of them have the same Eu^{2+} doping of 10%; it shows that pure Ba–S phase can be synthesized, but pure Sr–S phase can not be obtained by heating at 1650 °C. The Sr–S phase was reported to be synthesized by hot-pressing sintering (35 MPa) at 1800 °C,[7] and it seems that pure Sr–S phase could not be prepared under normal pressure and lower temperature. Fortunately, we found that the addition of only 1 wt % Ba (based on Sr concentration) was enough to stabilize the Sr–S phase, and a pure S phase could be obtained, as shown in curve a of Figure 1.

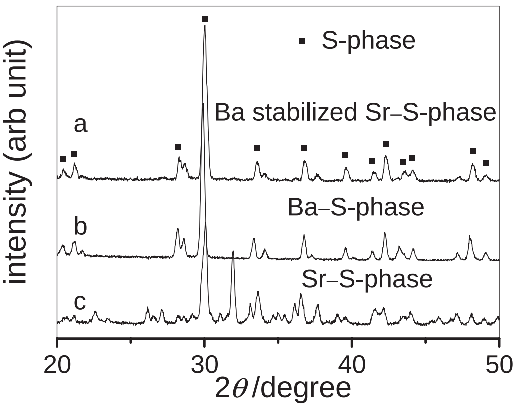

Figure 1. X-ray diffraction pattern of Ba-stabilized Sr–S phase, Ba–S phase, and Sr–S phase.

The result could be explained by the different structure of $Ba_2Al_2Si_{10}N_{14}O_4$ and $Sr_2Al_2Si_{10}N_{14}O_4$. As shown in Figure 2, although the tetrahedral framework of $Ba_2Al_2Si_{10}N_{14}O_4$ and $Sr_2Al_2Si_{10}N_{14}O_4$ is very similar, the Sr atom is coordinated by eight anions, but the Ba is coordinated by ten anions,[6] the Ba^{2+} is easier to enter the framework of S phase than Sr^{2+}. Because the $Ba_2Al_2Si_{10}N_{14}O_4$ and $Sr_2Al_2Si_{10}N_{14}O_4$ have the same framework, in the sintering process, the

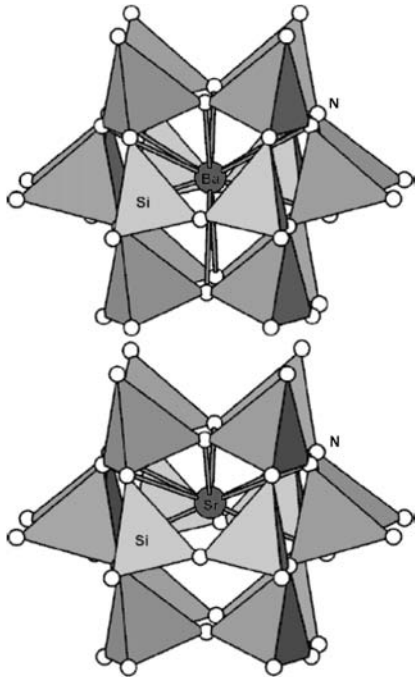

Figure 2. Structure of Ba–S phase and Sr-doped S phase.[6]

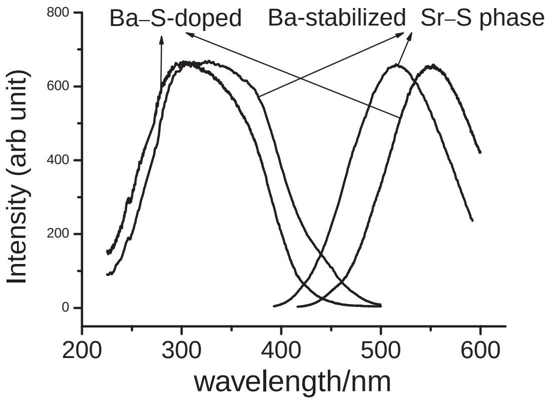

Figure 3. Excitation and emission spectrum of $Sr_{1.78}Ba_{0.02}Eu_{0.2}Al_2Si_{10}N_{14}O_4$ and $Ba_{1.8}Eu_{0.2}Al_2Si_{10}N_{14}O_4$.

$Ba_2Al_2Si_{10}N_{14}O_4$ crystal that formed first can play a role of seed to promote the formation of $Sr_2Al_2Si_{10}N_{14}O_4$. That is why Ba can stabilize $Sr_2Al_2Si_{10}N_{14}O_4$.

The excitation and emission spectra of both Eu^{2+}-doped Ba–S phase and Ba-stabilized Sr–S phase are shown in Figure 3. The peak of excitation band of Ba–S phase locates at about 330 nm, but the emission band of usually used UVLED is at about 365 nm, so the excitation of $Ba_{1.8}Eu_{0.2}Al_2Si_{10}N_{14}O_4$ does not match with this emission band of UVLED. The shift of excitation band to near 365 nm is necessary for the application of this phase in UVLED. As also could be seen in Figure 3, the Ba-stabilized Sr–S phase has a broad excitation spectrum from 300 to 370 nm, which covers the emission band of UVLED. The difference between excitation and emission may be ascribed to the lattice distortion caused by the replacement of Ba^{2+} with Sr^{2+}. It could be seen from Figure 1 that XRD peaks of Ba-stabilized Sr–S phase slightly shift to high angles compared with those of Ba–S phase, implying the decrease of lattice parameters. When the Eu occupies the site of Ba or Sr, the different Eu–N bond distance changes the crystal field and shrinks the lattice.

Figure 4 shows the fluorescence emission spectrum of $Sr_{1.98-x}Ba_{0.02}Eu_xAl_2Si_{10}N_{14}O_4$ ($x = 0.1$–0.5) sample with different Eu^{2+} concentrations. The emission band consists of a single intense broad emission band centered at 508–538 nm. The emission band is mainly attributable to the allowed $4f^65d$–$4f^7$ transition of Eu^{2+} ion. Red shift of the emission band from 508 to 538 nm is observed when the Eu^{2+} concentration is increased from 0.1 to 0.5. The 5d state is outmost excited state of Eu^{2+}, so when the Eu^{2+} concentration changed the alteration of the covalency and crystal field will affect the 5d state, the splitting of 5d state leads to the energy shift of $4f^65d$–$4f^7$ transition. Another feature shown in Figure 4 is the emission intensity as a function of the Eu^{2+} concentration. The emission intensity starts at low Eu^{2+} concentration then rises to maximum at a Eu^{2+} concentration of $x = 0.2$ and fall again. This change of emission intensity can be explained by concentration quenching which is mainly caused by the energy transfer between Eu^{2+} ions. When the concentration of Eu^{2+} increases, the emission from $4f^65d$ to $4f^7$ transition of Eu^{2+} increases, but the smaller distance between Eu^{2+} ions leads to the increased energy transfer between Eu^{2+} but the energy of radiation is decreased, so the emission intensity decreases. When the balance of these two opposition changes of energy are set up, the emission intensity will rise to the maximum, the emission intensity will decline when the energy transfer between Eu^{2+} beyond the energy of radiation. These two features imply that the luminescence properties of Eu^{2+}-doped S phase can be tailored by controlling the Eu^{2+} concentration. It is valuable for the industrial application.

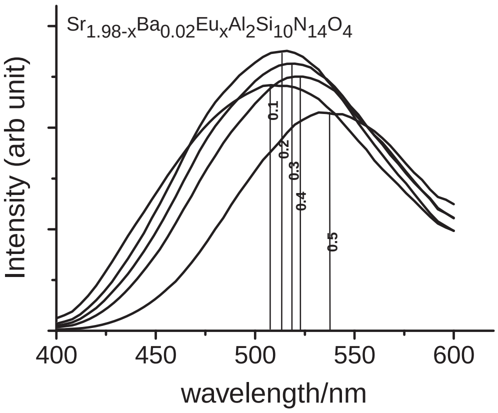

Figure 4. Photoluminescence emission spectrum of Eu^{2+}-doped Ba-stabilized Sr–S phase with different Eu^{2+} concentrations ($x = 0.1$–0.5). The excitation wavelength is 365 nm.

In this study, the stabilization effect of Ba on the structure of Sr–S phase has been discovered, the novel Eu^{2+}-doped Ba-stabilized $Sr_2Al_xSi_{12-x}N_{16-x}O_{x+2}$ green phosphor has a broad excitation band peak at 300–370 nm and emission maximum at about 514 nm, indicating that it is suitable for UVLED-based white light.

This research was supported by the National Natural Science Foundation of China (Grant no. 50702056) and by Chinese Academy of Sciences under the Hundred Talents Program. The first and second authors have equal contribution.

References

1 K. Sakuma, K. Omichi, N. Kimura, M. Ohashi, D. Tanaka, N. Hirosaki, Y. Yamamoto, R. J. Xie, T. Suehiro, *Opt. Lett.* **2004**, *29*, 2001.
2 Y. Q. Li, J. E. J. van Steen, J. W. H. van Krevel, G. Botty, A. C. A. Delsing, F. J. DiSalvo, G. de With, H. T. Hintzen, *J. Alloys Compd.* **2006**, *417*, 273.
3 J. W. H. van Krevel, J. W. T. van Rutten, H. Mandal, H. T. Hintzen, R. Metselaar, *J. Solid State Chem.* **2002**, *165*, 19.
4 R. J. Xie, N. Hirosaki, M. Mitomo, T. Suehiro, X. Xu, H. Tanaka, *J. Am. Ceram. Soc.* **2005**, *88*, 2883.
5 X. Xu, T. Nishimura, Q. Huang, R. J. Xie, N. Hirosaki, H. Tanaka, *J. Am. Ceram. Soc.* **2007**, *90*, 4047.
6 S. Esmaeilzadeh, J. Grins, Z. Shen, M. Eden, M. Thiaux, *Chem. Mater.* **2004**, *16*, 2113.
7 Z. Shen, J. Grins, S. Esmaeilzadeh, H. Ehrenberg, *J. Mater. Chem.* **1999**, *9*, 1019.